Available online at www.sciencedirect.com
ScienceDirect
Acta Materialia 57 (2009) 257–266
Acta MATERIALIA
www.elsevier.com/locate/actamat

Size-dependent shear fracture and global tensile plasticity of metallic glasses

F.F. Wu [a,b], Z.F. Zhang [a,*], S.X. Mao [a,c]

[a] Shenyang National Laboratory for Materials Science, Institute of Metal Research, Chinese Academy of Sciences, 72 Wenhua Road, Shenyang 110016, China
[b] School of Materials and Chemical Engineering, Liaoning University of Technology, 169 Shiying Street, Jinzhou 121001, China
[c] Department of Mechanical Engineering and Materials Science, University of Pittsburgh, 648 Benedum Hall, Pittsburgh, PA 15261, USA

Received 19 June 2008; received in revised form 5 September 2008; accepted 8 September 2008
Available online 1 October 2008

Abstract

The tensile ductility or brittleness of metallic glasses is found to depend strongly on the critical shear offset. Based on experimental observations, the tensile shear fracture processes of metallic glasses can be divided into three stages: multiplication and coalescence of the free volume, formation of void and the final fast propagation of a shear crack. Accordingly, the size effect on the tensile shear deformation processes of metallic glass can be well understood: with decreasing specimen size smaller than the equivalent critical shear offset, the shear deformation of metallic glass is changed from unstable to stable, which leads to a transition from global brittleness on the macroscale to large global plasticity or even necking on the microscale. These results are fundamentally useful in understanding the physical nature of tensile shear deformation of various metallic glasses and even in the design of new metallic glass materials with good plasticity.

Keywords: Metallic glasses; Shear band; Plastic deformation; Tensile plasticity; Critical shear offset

1. Introduction

Metallic glass, characteristic of high strength and hardness, is regarded as a potential candidate material in engineering fields [1–3]. However, there is a fatal weakness that impedes it from being used thus: its almost zero plasticity under tension and limited plasticity under compression [4–6]. Therefore, how to improve the plasticity of metallic glass has become one of the hottest topics in recent years. Although there have been many reports on the large compressive plasticity of some metallic glasses [7–14], tensile plasticity has seldom been observed [15]. As usually observed on the macroscopic scale, metallic glasses are often seen as brittle materials because their deformation only takes place at a few localized shear bands under compression or at a single shear band under tension, before exhibiting catastrophic failure [16]. On the microscopic scale, however, most metallic glasses can be regarded as ductile materials because individual shear bands can accommodate plastic strain as high as 10^2–10^4% [16–18]. Many investigations have thus been conducted to try to produce macroscopic plasticity in metallic glasses. Recently, based on the finding of a correlation between the fracture energy of metallic glasses and their elastic properties [19], a new method has been used to produce compositions for metallic glasses with appropriate elastic constants and thus enhance the macroscopic plasticity [7,10].

On the other hand, it is well known that some metallic glass composites with in situ dendrites possess considerable tensile plasticity [15,20,21], which is regarded as a milestone in the development of metallic glasses used as engineering materials. As pointed out by Hofmann et al. [20], the improvement in the large tensile plasticity and toughness of their metallic glass composites was based on two

* Corresponding author.
E-mail address: zhfzhang@imr.ac.cn (Z.F. Zhang).

1359-6454/$34.00
doi:10.1016/j.actamat.2008.09.012

principles: (i) introducing soft elastic/plastic inhomogeneities into a metallic glass matrix to initiate local shear banding around the inhomogeneities; and (ii) matching microstructural length scales to the characteristic length scale for plastic shielding of an opening crack tip to limit shear band extension, suppress shear band opening and avoid crack development. Hofmann et al.'s success in producing fracture toughness and tensile plasticity in metallic glass seems to have reignited the search for new metallic glasses with good performance properties. However, the reports above are the few credible experimental observations on tensile plasticity occurring in bulk metallic glasses [15,20]. For those metallic glasses even with super-high compressive plasticity, unfortunately, there is no clear experimental evidence to show tensile plasticity [7–11]. Recently, and surprisingly, a report has been published on the tensile plasticity in monotonic metallic glass [22] that shows the samples with gauge dimensions of about $100 \times 100 \times 250\ nm^3$ can display clear tensile plasticity as high as 23–45% through both uniform elongation and stable shear deformation. Meanwhile, a large equivalent plastic strain has been achieved in a metallic glass under biaxial tension [23]. These facts indicate that the nature of tensile deformation for various metallic glass materials has not been well understood. In this paper, we will clarify the tensile shear fracture processes of metallic glasses with different dimensions and microstructures, and try to fundamentally understand the tensile plasticity or brittleness of metallic glasses.

2. Experimental procedure

Ingots with compositions of $Zr_{52.5}Cu_{17.9}Al_{10}Ni_{14.6}Ti_5$ and $Zr_{56.2}Ti_{13.8}Nb_{5.0}Cu_{6.9}Ni_{5.6}Be_{12.5}$ were prepared by plasma arc melting a mixture of pure elements in a Ti-gettered argon atmosphere on a water-cooled copper plate. The ingots were then remelted several times to ensure their compositions were homogeneous. The microstructures and the phases of the prepared ingots were characterized with an LEO Supra 35 scanning electron microscope (SEM), together with a Rigaku X-ray diffractometer using Cu Kα radiation. The $Zr_{52.5}Cu_{17.9}Al_{10}Ni_{14.6}Ti_5$ ingot was identified as monolithic metallic glass by X-ray diffractometry (XRD), as shown in Fig. 1. The $Zr_{56.2}Ti_{13.8}Nb_{5.0}Cu_{6.9}Ni_{5.6}Be_{12.5}$ ingot was a metallic glass composite, and its XRD pattern is indicated in Fig. 1. The isolated islands phase (~25% in volume) corresponds to β-Zr-type dendrites with a body-centered cubic (bcc) structure, which are homogeneously dispersed in the metallic glass matrix (~75 vol.%).

By using SEM electron microprobe analysis, the compositions of the glass matrix and dendrites was determined to be $Zr_{47}Ti_{12.9}Nb_{2.8}Cu_{11}Ni_{19.6}Be_{16.7}$ and $Zr_{71}Ti_{16.3}Nb_{10}Cu_{1.8}Ni_{0.9}$, respectively. The dendrite axes had a length range of 20–60 μm. In addition, a regular pattern of secondary dendrite arms with spacing of 2–3 μm was observed. The volume fraction and size of the dendrites were measured on the cross-section surface of the plate. It was found that the volume fraction and size of the dendrites are basically constant over the thickness of the ingot.

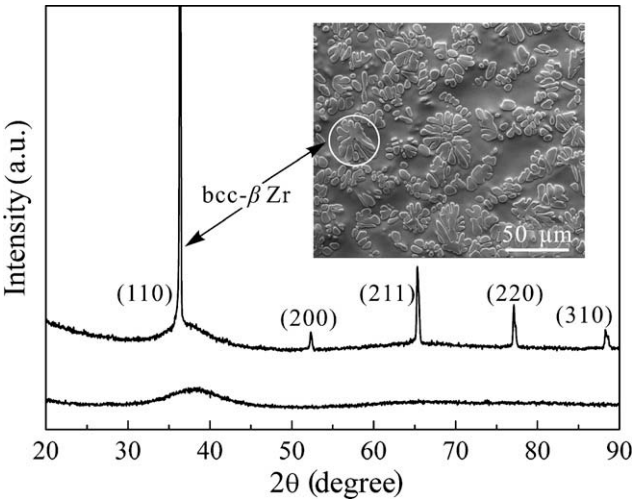

Fig. 1. XRD patterns of the bulk $Zr_{52.5}Cu_{17.9}Al_{10}Ni_{14.6}Ti_5$ metallic glass and the bulk bcc-β dendrite-reinforced metallic glass composite. Inset is an SEM image of the dendrite-reinforced metallic glass composite; the isolated islands are the bcc-β Zr dendrites.

Bulk tensile specimens of $Zr_{52.5}Cu_{17.9}Al_{10}Ni_{14.6}Ti_5$ and $Zr_{56.2}Ti_{13.8}Nb_{5.0}Cu_{6.9}Ni_{5.6}Be_{12.5}$ metallic glass materials with gauge dimensions of $1.5 \times 3.0 \times 10\ mm^3$ and a total length of 40 mm were prepared using electric spark machining and finally polished with 1.5 μm diamond paste. Meanwhile, medium-sized tensile specimens of $Zr_{52.5}Cu_{17.9}Al_{10}Ni_{14.6}Ti_5$ metallic glass with gauge dimensions of $0.017 \times 0.78 \times 4.0\ mm^3$ were carefully prepared by mechanical polishing. Uniaxial tensile tests were performed with a constant strain rate of about $1 \times 10^{-4}\ s^{-1}$ under an MTS810 testing machine at room temperature. Finally, the effective dimensions of three-point bending specimens are $0.5 \times 3.0 \times 10\ mm^3$, and the tests were conducted on $Zr_{52.5}Cu_{17.9}Al_{10}Ni_{14.6}Ti_5$ metallic glass with a constant cross-head displacement rate of $0.075\ mm\ s^{-1}$. After the mechanical tests, the specimens were observed by SEM and transmission electron microscopy (TEM) to reveal the deformation features.

3. Experimental results

3.1. Tensile deformation and fracture of a bulk metallic glass specimen

Fig. 2 shows the deformation features of the $Zr_{52.5}Cu_{17.9}Al_{10}Ni_{14.6}Ti_5$ metallic glass subjected to tensile loading. The bulk tensile specimen failed by a single shear fracture, with a shear fracture angle of about 56°, as shown in Fig. 2(a). From the fracture surface edge, it can be seen that there is a smooth region ranging over 20 μm in length, which is the typical shear offset caused by the formation and propagation of the main shear band (see Fig. 2(b) and (c)). It is noted that the smooth region is invisible on

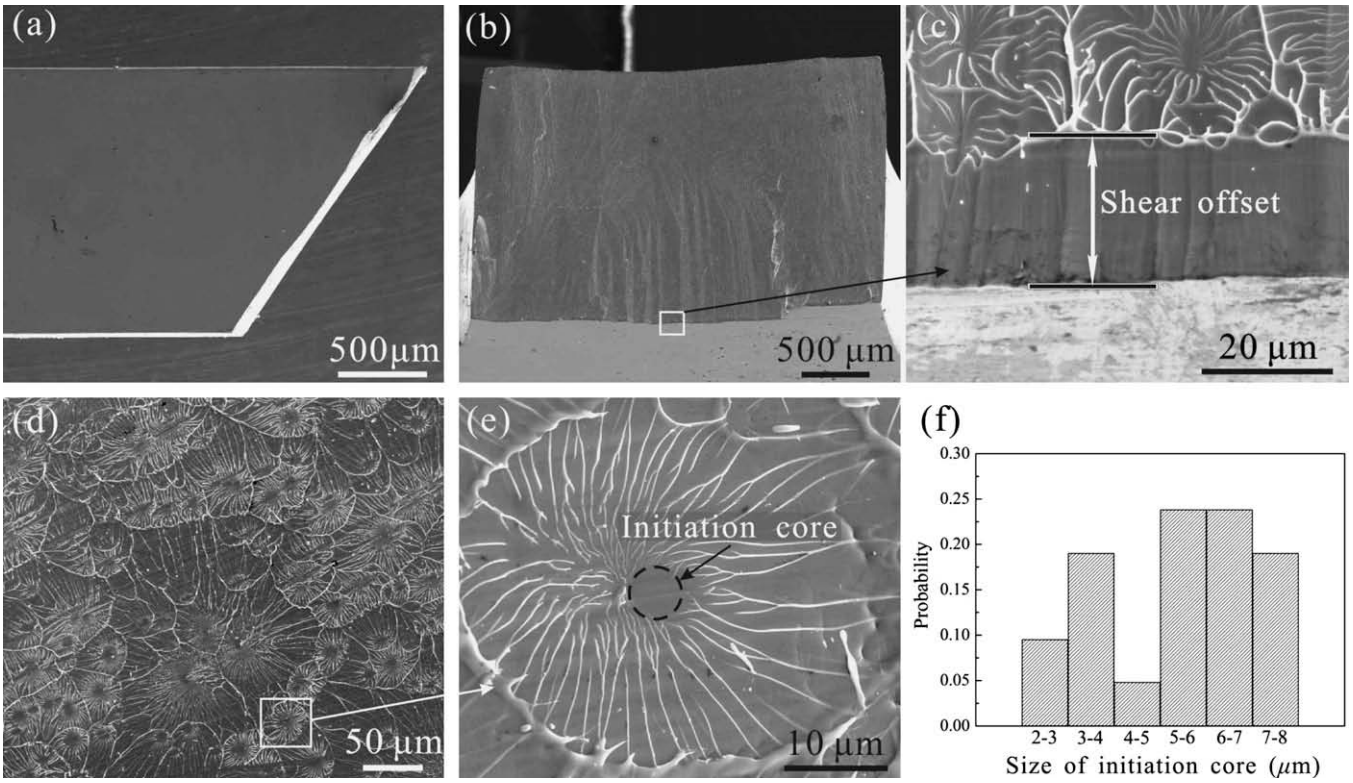

Fig. 2. SEM images of the tensile fracture features in the bulk $Zr_{52.5}Cu_{17.9}Al_{10}Ni_{14.6}Ti_5$ metallic glass. (a) The macroscopic fracture feature on the lateral surface. (b) The macroscopic feature of the fracture surface. (c) A higher magnitude SEM image showing the initial smooth shear region in the fracture surface. (d) The tensile fracture surface with many radiating cores. (e) A higher magnitude SEM image showing the core and the radial vein-like pattern in detail. (f) The core sizes measured on the tensile fracture surface of the Zr-based metallic glass.

the opposite edge of the fracture surface in Fig. 2(b), but it is visible on the opposite edge of the other fractured part of the specimens. By careful observation, we found that all the tensile or compressive specimens with shear offset before failure show only a smooth region in the shear offset. However, the specimens after failure always show both a smooth region and vein-like patterns. Due to the different stress states applied in specimens with different thicknesses, many crystalline metallic materials display shear lips or a flat fracture region in the fracture surface. However, for metallic glass, we found that the thickness of the specimens never changed the shear fracture characteristics. Whether in a plane stress or plane strain state, specimens always failed by shear fracture. Therefore, we think the width of the smooth region is equal to the shear offset that occurs before catastrophic failure by stable propagation of the shear band. Fig. 2(d) shows the inner region of the tensile fracture surface of the metallic glass, which is covered by many radial vein patterns [5]. A high-resolution SEM image (Fig. 2(e)) shows that the radial vein pattern is composed of a smooth core and an outer radial vein line [24]. The size distribution of the smooth cores is presented in Fig. 2(f). It can be seen that the size ranges from 2 to 8 μm, with a mean of about 5.5 μm. From the center of the core to the outer edge of the radial vein pattern, the mean distance is about 17.4 μm. The outer vein pattern becomes coarser with increasing distance away from the smooth core center [5,24]. In particular, it is interesting to find that the density of the cores on the whole fracture surface is as high as $1.06 \times 10^9\ m^{-2}$.

As is well known, shear bands are those areas of intense local plasticity separating undeformed sections of material which have displaced relatively to one another. Since the shear bands are only about 10–20 nm thick [16–18], they are not easily observed on the sample surface. Normally, the shear bands appear in the form of surface steps (defined here as the shear offset λ [25]) created by the relative shear displacement across the thin layer of the deformed material, with a shear angle of $\theta = 56°$ [5]. Given that the gauge of the tensile specimen is about 10 mm, the single shear offset contributes only 0.1% plasticity to the whole tensile specimen for the $Zr_{52.5}Cu_{17.9}Al_{10}Ni_{14.6}Ti_5$ metallic glass, which is consistent with the zero macroscopic tensile plasticity that has been widely observed in various metallic glasses [5,16,24,26,27].

3.2. Tensile deformation and fracture of a medium-sized metallic glass specimen

As indicated above (Fig. 2(c)), there are two typical regions with different patterns in the tensile fracture surfaces of the bulk metallic glass specimen, namely the smooth region without radial vein patterns at the very edge of the fracture surface and the region with radial vein

patterns following the smooth region. It is proposed that the smooth region should be related to the stable shear deformation. Furthermore, it is envisioned that there would be only a smooth region without vein patterns on the fracture surface when the metallic glass specimen is thinner than a critical size, indicating that the radial vein pattern will disappear completely. To this end, a number of medium-sized specimens with gauge dimensions of $0.017 \times 0.78 \times 4.0\,mm^3$ were made from the bulk $Zr_{52.5}Cu_{17.9}Al_{10}Ni_{14.6}Ti_5$ metallic glass which were then subjected to tensile loading. From Fig. 3, it is clear that shear fracture also occurred in the medium-sized metallic glass specimen. However, unlike the bulk specimen, its fracture surface showed a fully smooth region without any vein pattern, as well as triple-point veins at the very edge of the surface. The smooth region should be a stable shear stage of the tensile deformation process, and the triple-point veins result from the fast rupture of the two parts of the tensile specimen during the final stage of the tensile deformation process. A similar morphology was often observed on the fracture surfaces of metallic glass ribbon with dimensions similar to those previously reported [28,29]. The difference in the fracture surfaces between the bulk specimen and the medium-sized specimen will be discussed in Section 4.

3.3. Tensile deformation and fracture of bulk metallic glass composite

The ductile dendrite-reinforced $Zr_{56.2}Ti_{13.8}Nb_{5.0}Cu_{6.9}Ni_{5.6}Be_{12.5}$ metallic glass composite can be regarded as a combination of numerous small metallic glass matrices with ductile dendrites. Therefore, unlike the bulk monolithic composite, there should be no radial vein pattern on the tensile fracture surfaces. Fig. 4 shows the tensile stress–strain curves of the bulk specimens of $Zr_{52.5}Cu_{17.9}Al_{10}Ni_{14.6}Ti_5$ metallic glass and the $Zr_{56.2}Ti_{13.8}Nb_{5.0}Cu_{6.9}Ni_{5.6}Be_{12.5}$ metallic glass composite at room temperature. It is found that the monolithic metallic glass failed at a maximum stress of 1723 MPa by the propagation of a single shear band, as shown in Fig. 2(a). There is no macroscopic tensile plasticity and the fracture surface makes an angle of about 56° with respect to the tensile stress axis, which can be explained by the unified tension criterion [30]. The fractography was described in Section 3.1. However, the metallic glass composite exhibits an initial elastic deformation behavior with an elastic strain of about 1.7%, and then begins to yield at about 1365 MPa, followed by a slight strain hardening up to about 1432 MPa with a tensile plastic strain of 1.8%, as shown in Fig. 4. Its tensile fracture stress is 1364 MPa, which is smaller than that of the monolithic metallic glass. Further investigation indicates that necking appeared near the fracture region and profuse shear bands were formed in the metallic glass composite, as displayed in Fig. 5(a). Due to the constraint of the dendrites, multiple and even intersected shear bands were formed, as shown in Fig. 5(b). Moreover, the vein patterns on the fracture surface of the metallic glass composite are very different from those in the monolithic one (see Fig. 2(c)–(e)). The vein patterns are no longer radial in shape, and there are no smooth cores in the vein patterns, as shown in Fig. 5(c). Careful observation indicated that some regions are still smooth, which is similar to that observed in the medium-sized metallic glass specimen, as shown in Fig. 5(d). These results demonstrate that the fracture surface of the metallic glass composite is characterized by a combination of the features of the bulk and medium-sized metallic glass specimens.

4. Discussion

4.1. Tensile fracture processes of metallic glass

As is well known, the plastic deformation of metallic glass at room temperature is produced by the shear offset or shear displacement of two undeveloped parts separated by the localized shear band [16]. With the shear band propagating, the shear offset increases, resulting in local plastic deformation. When a shear band propagates to a critical

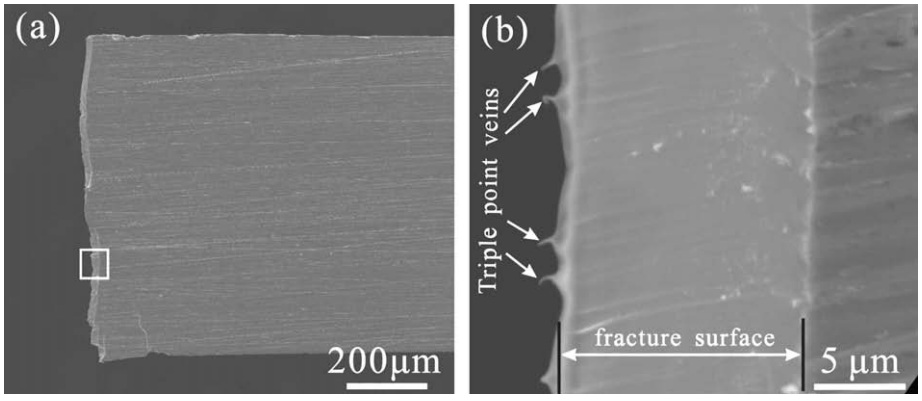

Fig. 3. (a) The tensile fracture feature of the medium-sized $Zr_{52.5}Cu_{17.9}Al_{10}Ni_{14.6}Ti_5$ metallic glass specimen. (b) The fully smooth shear region in the tensile fracture surface of medium-sized metallic glass specimen.

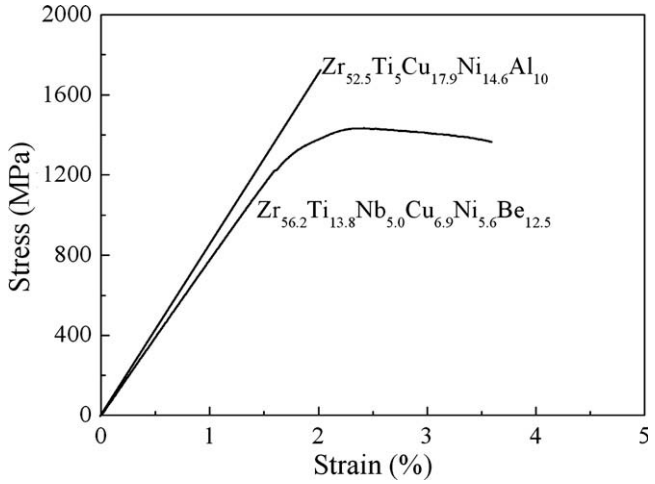

Fig. 4. Tensile stress–strain curves of the bulk $Zr_{52.5}Cu_{17.9}Al_{10}Ni_{14.6}Ti_5$ metallic glass (marked with A) and the $Zr_{56.2}Ti_{13.8}Nb_{5.0}Cu_{6.9}Ni_{5.6}Be_{12.5}$ metallic glass composite (marked with B).

length, it develops steadily with a low bonding strength [31] so that the final catastrophic fracture always proceeds along the shear band. Thus, there should be a "largest shear offset" or "critical shear offset (λ_c)" above which the shear band becomes unstable, leading to the final shear fracture [18]. The critical shear offset is a parameter directly reflecting the stable shear capability. The length of the critical shear offset should be equal to the size of the smooth region at the initial fracture surface of metallic glass sample after deformation [18,32]. Therefore, it is suggested that the shear deformation capability of a metallic glass is related to its critical shear offset: the local plastic strain of the metallic glass at fracture increases with increasing critical shear offset.

Therefore, based on the present observations and the analysis above, a landscape is proposed to understand the physical nature of the tensile shear fracture processes in the $Zr_{52.5}Cu_{17.9}Al_{10}Ni_{14.6}Ti_5$ bulk metallic glass specimen, as shown schematically in Fig. 6. There are three stages during the fracture processes: (I) the multiplication of free volume; (II) the coalescence of free volume and formation of void; and (III) the final fast propagation of a shear crack.

In stage I, the shear band starts to form and propagates stably, with a continuous increase in the free volume within the shear band. Thereby, the density of the free volume increases and the resistance to shear deformation within the shear bands decreases. Since some voids have been observed in the deformed regions using TEM, it has been speculated that the formation of these voids should result from the coalescence of the excess free volume once flow stops [33–35]. As the free volume increases, the free energy of the shear band with respect to the bulk sample also increases. The excess free energy within the shear band can be correlated with a free volume chemical potential that provides a driving force for void nucleation during

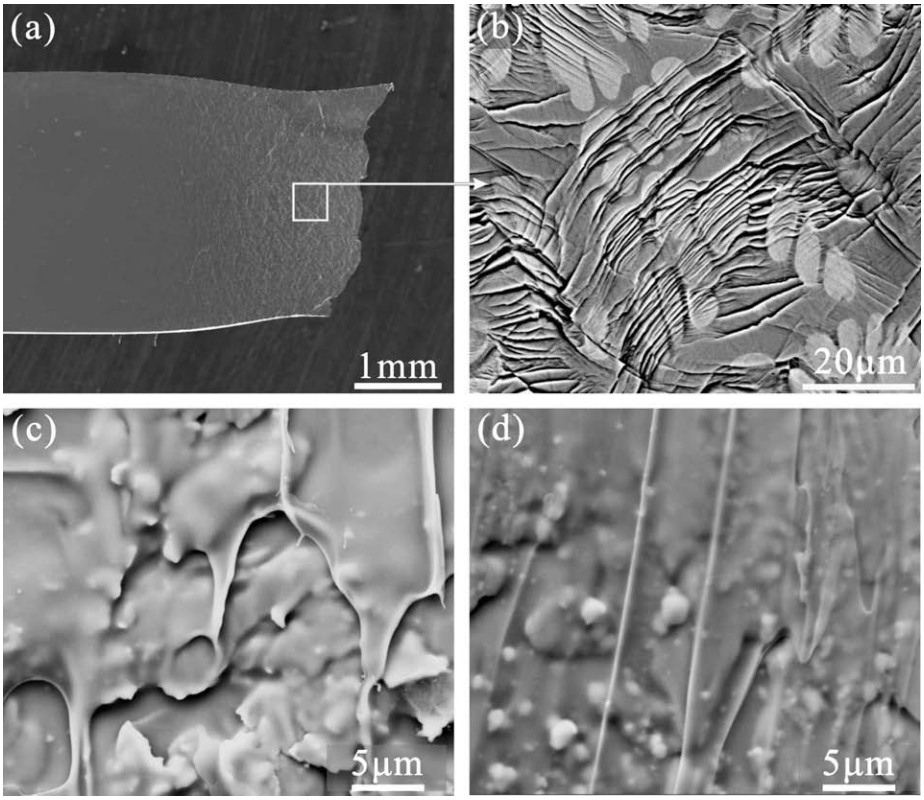

Fig. 5. (a) Considerable plastic strain and necking undergone by the bulk $Zr_{56.2}Ti_{13.8}Nb_{5.0}Cu_{6.9}Ni_{5.6}Be_{12.5}$ metallic glass composite. (b) Profuse shear bands forming on the lateral surface of the bulk metallic glass composite. (c and d) Vein patterns observed on the fracture surface of the bulk metallic glass composite.

shear deformation of metallic glasses due to free volume coalescence [36]. In tension, the growth of voids would be promoted by a normal tensile stress [5,24], perhaps resulting in premature fracture.

In stage II, when the shear offset increases up to the threshold shear offset (λ_{th}), the shear band develops steadily and the free volume coalesces. The voids then start to induce the formation of a local crack, and the shear crack propagates slowly and stably.

In stage III, the shear offset reaches the critical value (about 20 μm for the present Zr-based metallic glass) and the core size (crack length) is about 5.5 μm. Based on the fracture mechanism of materials incapable of plastic deformation [37], the maximum tensile stress of the Zr-based metallic glass at the crack tip is illustrated in Fig. 7, and can be calculated by

$$\sigma_{max} = \frac{2w/\sin^2\theta}{w\sin\theta - \lambda_c}\frac{1}{1-\left(\frac{c}{D}\right)^2}\left(\frac{c}{2\rho}\right)^n \sigma_f \quad (1)$$

Here, w is the transverse length of the specimens, $\theta = 56°$ is the shear angle [24], λ_c is the critical shear offset, σ_f is the nominal tensile fracture stress, c is the diameter of the crack, D is the diameter of the vein pattern, ρ is the radius of the crack tip and n is the stress concentration index, which reflects the ability of stress concentration. For a crack in ideal brittle material, the stress concentration index $n = 0.5$ [37]; however, for a shear band in metallic glass, $0 < n < 0.5$. If considering $w = 1500$ μm (1.5 mm), $\theta = 56°$, $\lambda_c = 20$ μm, $\sigma_f = 1.66$ GPa [24], $c = 5.5$ μm, $D = 34.8$ μm, $\rho = 10$ nm (half the thickness of the shear band [38]) and $n = 0.2$, then the maximum tensile strength at the crack tip is calculated to be about $\sigma_{max} = 18.7$ GPa, which is very close to the theoretical strength of metallic glass (i.e. $E/5 = 17.7$ GPa [37,39]). Thus, the crack propagates fast, leading to the catastrophic brittle failure of the tensile specimen, leaving many radiating vein patterns on the fracture surfaces due to local melting [5,16,24].

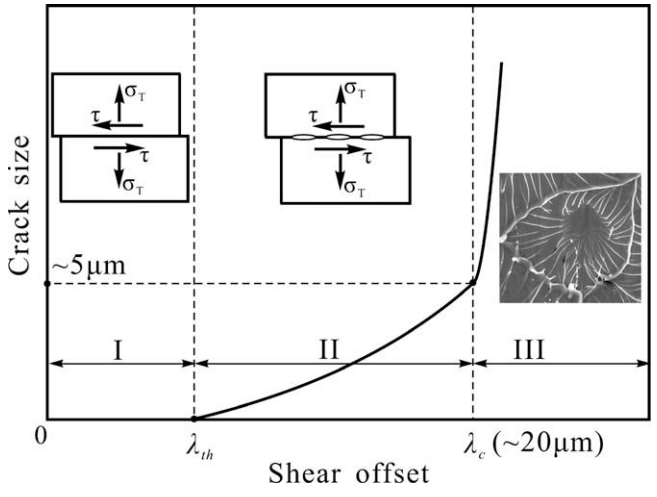

Fig. 6. Illustration of the crack size as a function of shear offset, showing the three stages in the tensile fracture processes of the $Zr_{52.5}Cu_{17.9}Al_{10}Ni_{14.6}Ti_5$ metallic glass: region I, the multiplication of free volume; region II, the coalescence of free volume and formation of void; region III, the final fast propagation of shear crack.

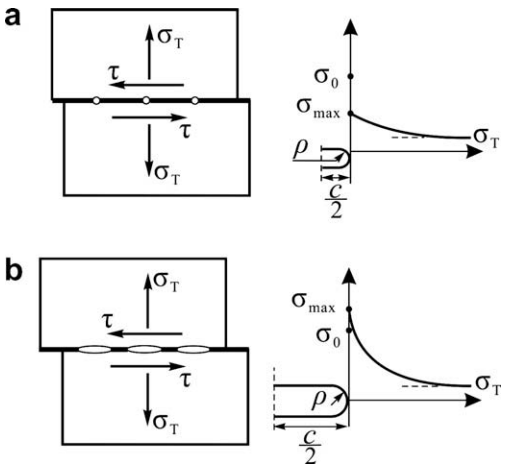

Fig. 7. The tensile stress in the region adjacent to an elliptical crack in the shear band of a metallic glass. (a) The tensile stress in the crack tip is lower than the theoretical strength of the metallic glass. (b) The tensile stress in the crack tip is larger than the theoretical strength of the metallic glass.

Due to the catastrophic failure (tensile instability), it is difficult to observe the propagation of the shear band in metallic glass. However, bending produces an inherently inhomogeneous stress state in which the shear band is arrested by the gradient in the applied stress. Therefore, the propagation of the shear band can be clearly observed in the tensile side of the metallic glass bending specimens. Fig. 8 is a typical deformation feature on the tensile side of the $Zr_{52.5}Cu_{17.9}Al_{10}Ni_{14.6}Ti_5$ metallic glass specimen subjected to a bending test. It is clear that cracks have been formed within the shear bands, which should correspond to stage II of the shear banding process mentioned above.

4.2. Geometric effect on the tensile plasticity of metallic glass

On the one hand, the critical shear offset λ_c stands for the ability of stable propagation for a shear band under tension; on the other hand, the critical shear offset should be sensitive to the chemical composition and local short-range structure, such as the different bonding types of amorphous atoms [16]. For different metallic glasses, there are different critical shear offsets λ_c, depending on the fine details of the alloy compositions or atom bonding. For a tensile specimen, if the ratio of the gauge length L to the transverse width w is 2:1, the sum plastic strain due to the formation of multiple shear bands can be expressed as a function of the shear offset and specimen size

$$\varepsilon_p = \sum_{i=1}^{N}(\lambda_{ci}\cos\theta_i/2w) \quad (2)$$

Here, N is the number of shear bands, θ is the shear angle between the shear plane and the tensile direction and w is the transverse width at the gauge of the specimen. Considering that there is only one shear band, the maximum tensile plastic strain in Eq. (2) can be rewritten as

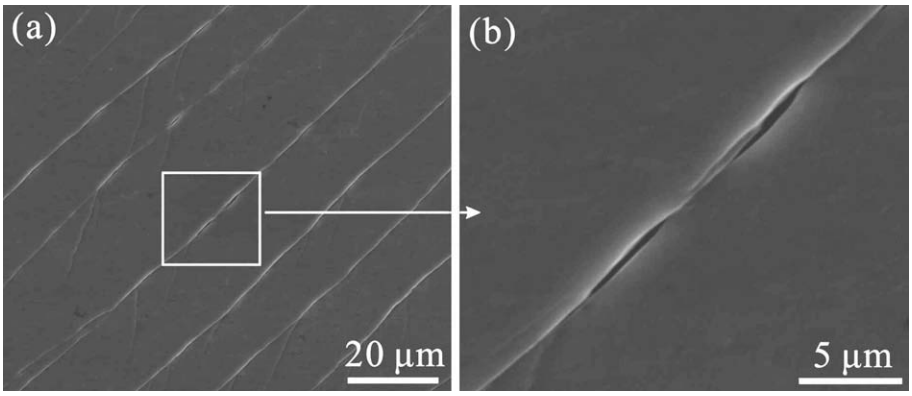

Fig. 8. (a) The shear bands formed in the tensile side of the bulk $Zr_{52.5}Cu_{17.9}Al_{10}Ni_{14.6}Ti_5$ metallic glass after bending. (b) A higher magnitude SEM image showing the cracks within the shear band.

$$\varepsilon_p = \lambda_c \cos\theta / 2w \tag{3}$$

According to the present experimental observations for the $Zr_{52.5}Cu_{17.9}Al_{10}Ni_{14.6}Ti_5$ metallic glass, it is known that $\lambda_c = 20$ μm and $\theta = 56°$ [24]. Therefore, Eq. (3) can be further simplified as

$$\varepsilon_p = 5.59/w \quad (\text{at } w > \lambda_c \sin\theta) \tag{4}$$

Here, the unit for w is μm. However, when the specimen size is equal to or smaller than the equivalent critical shear offset, i.e. $w \leqslant \lambda_c \sin\theta$, stable tensile shear deformation will occur continuously, as illustrated by stage II in Fig. 6 and region II in Fig. 9. The fully smooth fracture surface in the thin metallic glass specimen in Fig. 3 verified this analysis. Therefore, the maximum tensile plastic strain of metallic glass can be described as

$$\varepsilon_p = \lambda \cos\theta / 2w \tag{5}$$

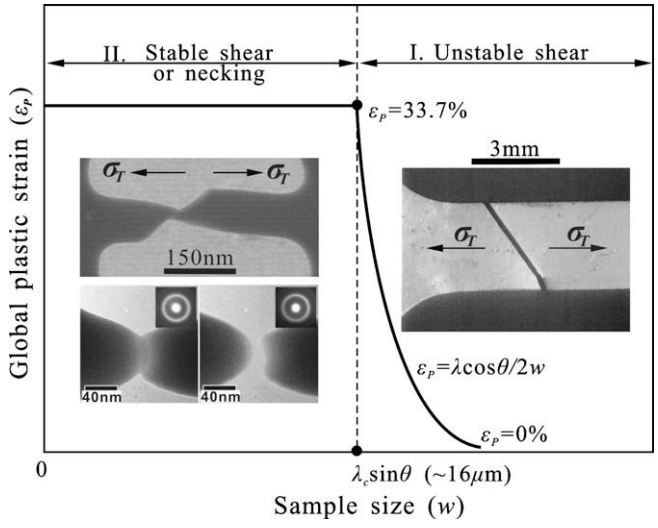

Fig. 9. Illustration of the size effect on the tensile plasticity or brittleness of metallic glass: region I, the unstable shear region at $w > \lambda_c \sin\theta$ (inset is the optical image of tensile specimen of metallic glass with large dimension [16]); region II, the stable shear region at $w \leqslant \lambda_c \sin\theta$ (insets are the typical stable shear and necking of the TEM in situ tensile specimen with a gauge dimension of ~100 nm × 100 nm × 250 nm [22]).

Substituting $w = \lambda \sin\theta$ and $\theta = 56°$ in Eq. (5), the maximum tensile plastic strain for the specimen with size smaller than the equivalent critical shear offset should be a constant, i.e.

$$\varepsilon_p = 33.7\% \tag{6}$$

The relationship between the tensile plasticity and the specimen size according to Eqs. (4) and (6) is illustrated in Fig. 9. The figure clearly shows the size effect on the macroscopically tensile plasticity or brittleness of the metallic glass at two different regions, i.e. the unstable shear and the stable shear or necking. In region I, since the specimen size w is significantly larger than the equivalent critical shear offset, i.e. $w > \lambda_c \sin\theta$, the tensile plasticity of metallic glass is a function of specimen size w due to the unstable shear without global plasticity, as shown in the right inset of Fig. 9. Therefore, the deformation of the metallic glass in region I is mainly characterized by catastrophically brittle failure, which corresponds to the fracture mechanism of bulk metallic glasses in previous reports [5,24]. In region II, the specimen size w is equal to or smaller than the equivalent critical shear offset, i.e. $w \leqslant \lambda_c \sin\theta$, so the shearing process should be stable up to the maximum tensile plasticity of about 33.7%, as in Eq. (6). During the in situ tensile experiments of small-sized metallic glass with dimensions of 100 nm × 100 nm × 250 nm, the stable shearing process or necking with a tensile plasticity of 23–45% was successfully observed [22], as shown in the left inset of Fig. 9. This result provides clear evidence that metallic glasses with dimensions smaller than the critical shear offset do have the stable shear ability to display global tensile plasticity. In addition to tensile deformation, the stable shear ability can also be applied to the compressive experiments of the brittle Mg-based metallic glasses, which often break fragmentally on the millimeter scale but fail by shear deformation on the micrometer scale [40]. In Zheng et al.'s work [40], the plasticity of the micrometer specimen was claimed to be a result of its defect-free nature on that small scale; however, we believe the great difference in plasticity between micrometer-scale and millimeter-scale specimens could be due to the small critical shear offset of the Mg-

based metallic glass and its large shear-cleavage coefficient of $\alpha = \tau_0/\sigma_0$ [30,41,42]. Therefore, the high tensile plasticity in the small-sized specimen is assumed to be that the specimen size is far smaller the equivalent critical shear offset, so the free volume accumulated does not reach the threshold amount to form large voids or cracks, as observed in Fig. 8(a) and (b).

On the other hand, due to the highly localized shear deformation in metallic glass, the elastic energy stored before fracture is mostly dissipated on the fracture surface as heat [43]. Some results have shown that heat plays an important role in the softening of a shear band and the catastrophic fracture of metallic glass [44]. The energy density of the shear fracture surface caused by the elastic energy release during the fracture process can be expressed approximately as [25,45]

$$\delta = \frac{1}{2}\sigma_e \varepsilon_e V/A = w\sigma_e\varepsilon_e \sin\theta \tag{7}$$

Here, σ_e is the maximum elastic stress (elastic limit), ε_e is the maximum elastic strain, V is the volume of the sample, A is the area of the main shear plane, w is the sample size (diameter or width) and θ is the shear angle between the shear plane and the loading direction. According to Eq. (7), it is clear that the elastic energy density dissipated on the shear fracture surface decreases linearly with decreasing sample size (w). Thus, a decreasing sample size will enhance the stability of the shear band, i.e. it becomes difficult to prevent the shear band from propagating enough to form a crack. Therefore, with decreasing sample size, it is easier for the less heat in the shear band to be distributed in neighboring space, and so the atoms diffuse in a relatively homogeneous manner. In this case, the multiplication of shear bands becomes more likely, thus enhancing the plasticity of the metallic glass.

4.3. Tensile plasticity of metallic glass composites

The shear band has been shown to be a weak location [31], so the uncontrolled propagation of a long shear band will lead to catastrophic failure. Therefore, it is an important principle for high tensile plasticity that the free propagation of active shear bands must be constrained. One effective way to do this is to introduce a second phase through an ex situ or in situ method [15,46]. As displayed in Fig. 5, dendrite particles reinforced the formation of multiple short shear bands in metallic glass composite remarkably even under tension loading. Short shear bands are very important in maintaining the global strength of the metallic glass and hence improve its plastic deformation ability, as illustrated schematically in Fig. 10(a). For a monolithic metallic glass, when an active shear band propagates through the tensile specimen, because the strength of the shear band (σ_S) is less than the strength of the undeformed metallic glass (σ_0) [31], the flow stress σ_f to drive the shear plastic deformation of the monolithic metallic glass should be controlled by σ_S rather than σ_0, as shown in Fig. 10(a). For the metallic glass composite with ductile dendrites, due to the dendrites blocking the shear bands, the length of the active shear band, λ, is far smaller than that in monolithic metallic glass, as indicated in Fig. 10(a). When the shear band is formed, the flow stress σ_f of the metallic glass composite can be controlled by both σ_S rather than σ_0 as

$$\sigma_f = \sigma_0 - \frac{\lambda\sin\theta}{w}(\sigma_0 - \sigma_S) \quad (0 < \lambda \leqslant w/\sin\theta) \tag{8}$$

Here, w and θ are the width of the specimen and the shear angle, respectively. From Eq. (1), when λ increases to $w/\sin\theta$, $\sigma_f = \sigma_S$, the monolithic metallic glass will fail catastrophically due to the rapid propagation of the weak shear band through the whole specimen. With the mean free propagation path λ decreasing, σ_f becomes close to σ_0, which is the reason why the shear strength of the metallic glass composite is only slightly lower than that of the metallic glass matrix even though the strength of shear band is one-fifth of that of the original metallic glass [31], as shown in Figs. 4 and 10(b). Therefore, dense short shear bands decrease the global strength of the metallic glass composite only slightly, which is important for the formation of more shear bands in as-yet-undeformed matrix. Due to the small loss in the global strength and the length of shear band λ being very close to the critical length λ_0 of the shear offset, considerable tensile plastic strain is achieved in the dendrite-reinforced metallic glass composite [15,20,41], as shown in Fig. 4. It is noted that the prop-

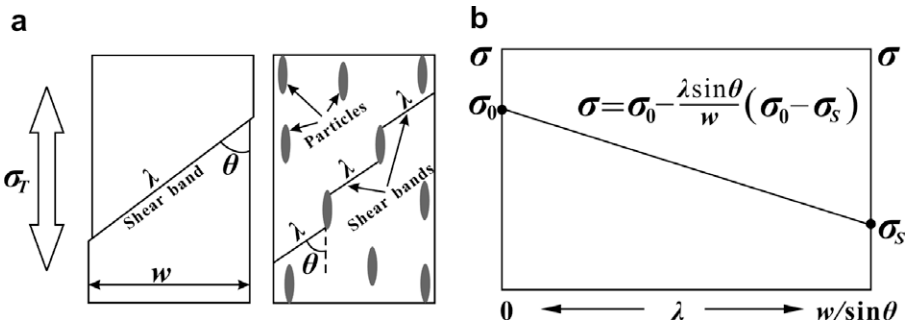

Fig. 10. (a) Illustration of the metallic glass and the dendrite-reinforced metallic glass composite under tensile loading. (b) Schematic illustration of the effective strength of a metallic glass decreasing monotonically with the length of shear band.

agation path of shear band is decided by the morphology of the second phase. Usually the metallic glass composites are reinforced by micrometer or even larger scale particles, which display only limited plastic deformation. However, in some reported novel metallic glass with excellent plasticity, there have been found to exist a large number of nanometer scale particles or inhomogeneities in the metallic glass matrix. Therefore the propagation path of the shear band should be on the nanometer scale, and the length of the active shear band is very close to the thickness λ_S of the shear band, leading to the serious deflection, multiplication and intersection of the shear bands and large global plasticity [8,9]. The model presented in Eq. (8) is used simply to explain the function of the mean free propagation path of the shear band. If the whole composite is considered, the relatively weaker dendrites should be expected to reduce the strength of the whole composite. From the stress–strain curve, the work-hardening corresponds to the continuous yielding that occurs in the dendrites. When the plastic deformation of the dendrites accumulates to a certain level, the shear bands will be activated in the interface between the dendrites and the matrix. Meanwhile, the dendrites can prevent the free propagation of shear bands, so multiple shear bands are activated.

Recently, numerous efforts have been made to improve the plasticity or ductility of various metallic glasses. From this viewpoint, both multiple shear bands and stable shear deformation ability should be the premise of the considerable tensile plasticity for metallic glasses. The concept of the critical shear offset stands for the stable shear deformation or nature of shear banding capability, which should be useful in understanding and even designing metallic glass materials with some degree of tensile plasticity. For example, in the metallic glass foam reported by Brother et al. [47] and the metallic glass composite with dendrites reported by Hays et al. [15] or Hofmann et al. [20], the individual strut or separated part of the metallic glass matrix has dimensions of about 20 μm, which should be very close to the equivalent critical shear offset, so multiple shear bands and stable shear will contribute to the large plasticity either under compressive or even under tensile loading.

In addition, recent studies of micropillar specimens of metallic glasses have shown that there is no catastrophic failure under compression [48–50]. It is well known that intrinsic brittle metallic glasses generally fracture into fragments at the onset of yielding [51]. However, the micropillar specimens of Mg-based metallic glasses can afford some stable shear deformation under compression, exhibiting a degree of global plastic strain [49,50]. These results indicate size exerts a big effect on the plasticity of metallic glasses. From the concept of critical shear offset, these recent results on micropillar compressive specimens should be related to the reinforced stable shear deformation with decreasing sample size. Furthermore, a critical assessment of the recent reports on ductile metallic glasses with excellent plasticity [9,10,40,49,52] reveals that most of them were tested with a sample size between 1 and 2 mm. The main problem is that the comparison of the plasticity of different metallic glasses does not fit a single model; in particular, the data have not been recorded for the same sample size. However, the present findings indicate that the effect of sample size on the plasticity of metallic glass should be taken into account. Thus, the results reported in literature are often not strictly comparable.

5. Conclusions

The tensile fracture processes of metallic glass can be divided into three stages: multiplication and coalescence of the free volume; formation of voids; and the final fast propagation of shear crack. During tensile deformation, the critical shear offset is an important parameter directly characterizing the shear ability of metallic glass. In terms of the shear offset and its stability, the size effect on the tensile plasticity or brittleness in metallic glasses can be clearly understood. When the specimen size of metallic glass is larger than the equivalent critical shear offset, the shear deformation is unstable, leading to a brittle fracture; however, when the specimen size is smaller than the equivalent critical shear offset, the shear deformation should be stable up to the occurrence of certain tensile plasticity. The new concept on the stable shear ability should be helpful for a better understanding of the physical nature of tensile plasticity or brittleness in various metallic glasses, and even for designing new high-performance metallic glass materials with good plasticity in the future.

Acknowledgements

The authors acknowledge the stimulating discussion with Prof. M.L. Sui and Dr. H. Guo. This work was financially supported by the National Outstanding Young Scientist Foundation under Grant No. 50625103, the National Natural Science Foundation of China (NSFC) under Grant Nos. 50401019 and 50871117, the "Hundred of Talents Project" of the Chinese Academy of Sciences, and National Basic Research Program of China under Grant No. 2004CB619306.

References

[1] Johnson WL. MRS Bull 1999;24:42.
[2] Inoue A. Acta Mater 2000;48:279.
[3] Wang WH, Dong C, Shek CH. Mater Sci Eng R 2004;44:45.
[4] Xing LQ, Li Y, Ramesh KT, Li J, Hufnagel TC. Phys Rev B 2001;64:180201.
[5] Zhang ZF, Eckert J, Schultz L. Acta Mater 2003;51:1167.
[6] Zhang ZF, Zhang H, Pan XF, Das J, Eckert J. Philos Mag Lett 2005;85:513.
[7] Schroers J, Johnson WL. Phys Rev Lett 2004;93:255506.
[8] Das J, Tang MB, Kim KB, Theissmann R, Baier F, Wang WH, et al. Phys Rev Lett 2005;94:205501.
[9] Yao KF, Ruan F, Yang YQ, Chen N. Appl Phys Lett 2006;88:122106.
[10] Liu YH, Wang G, Wang RJ, Zhao DQ, Pan MX, Wang WH. Science 2007;315:1385.

[11] Yao KF, Zhang CQ. Appl Phys Lett 2007;90:061901.
[12] Shen J, Huang YJ, Sun JF. J Mater Res 2007;22:3067.
[13] Huang YJ, Shen J, Sun JF. Appl Phys Lett 2007;90:081919.
[14] Wu FF, Zhang ZF, Mao SX. J Mater Res 2007;22:501.
[15] Hays CC, Kim CP, Johnson WL. Phys Rev Lett 2000;84:2901.
[16] Pampillo CA. J Mater Sci 1975;10:1194.
[17] Chen H, He Y, Shiflet GJ, Poon SJ. Nature 1994;367:541.
[18] Wu FF, Zhang ZF, Jiang F, Sun J, Shen J, Mao SX. Appl Phys Lett 2007;90:191909.
[19] Lewandowski JJ, Wang WH, Greer AL. Philos Mag Lett 2005;85:77.
[20] Hofmann DC, Suh JY, Wiest A, Duan G, Lind ML, Demetriou MD, et al. Nature 2008;451:1085.
[21] Lee ML, Li Y, Schuh CA. Acta Mater 2004;52:4121.
[22] Guo H, Yan PF, Wang YB, Tan J, Zhang ZF, Sui ML, et al. Nat Mater 2007;6:735.
[23] Wu FF, Zhang ZF, Shen J, Mao SX. Acta Mater 2008;56:894.
[24] Zhang ZF, Eckert J, Schultz L. Metall Mater Trans A 2004;35:3489.
[25] Wu FF, Zhang ZF, Shen BL, Mao SX, Eckert J. Adv Eng Mater 2008;10:727.
[26] Liu CT, Heatherly L, Easton DS, Carmichael CA, Schneibel JH, Chen CH, et al. Metall Mater Trans A 1998;29:1811.
[27] Zhang ZF, Wu FF, He G, Eckert J. J Mater Sci Technol 2007;23:747.
[28] Matthews DTA, Ocelík V, Bronsveld PM, Hosson JTMD. Acta Mater 2008;56:1762.
[29] Megusar J, Argon AS, Grant NJ. Mater Sci Eng 1979;38:63.
[30] Zhang ZF, Eckert J. Phys Rev Lett 2005;94:094301.
[31] Bei H, Xie S, George EP. Phys Rev Lett 2006;96:105503.
[32] Pampillo CA, Chen HS. Mater Sci Eng A 1974;13:181.
[33] Donovan PE, Stobbs WM. Acta Metall 1981;29:1419.
[34] Li J, Spaepen F, Hufnagel TC. Philos Mag A 2002;82:2623.
[35] Li J, Wang ZL, Hufnagel TC. Phys Rev B 2002;65:144201.
[36] Wright WJ, Hufnagel TC, Nix WD. J Appl Phys 2003;93:1432.
[37] Courtney TH. Mechanical behaviour of materials. New York: McGraw-Hill; 1990.
[38] Zhang Y, Greer AL. Appl Phys Lett 2006;89:071907.
[39] Bian Z, Pan MX, Zhang Y, Wang WH. Appl Phys Lett 2002;81:4739.
[40] Zheng Q, Ma H, Ma E, Xu J. Scripta Mater 2006;55:541.
[41] Wu FF, Zhang ZF, Peker A, Mao SX, Eckert J. Phys Rev B 2007;75:134201.
[42] Zhang ZF, Eckert J. Adv Eng Mater 2007;9:143.
[43] Lewandowski JJ, Greer AL. Nat Mater 2006;5:15.
[44] Yang B, Liaw PK, Wang G, Morrison M, Liu CT, Buchanan RA, et al. Intermetallics 2004;12:1265.
[45] Wu FF, Zhang ZF, Mao SX. Philos Mag Lett, submitted for publication.
[46] Schuh CA, hufnagel TC, Ramamurty U. Acta Mater 2007;55:4067.
[47] Brothers AH, Dunand DC. Adv Mater 2005;17:484.
[48] Schuster BE, Wei Q, Ervin MH, Hruszkewycz SO, Miller MK, Hufnagel TC, et al. Scripta Mater 2007;57:517.
[49] Zheng Q, Cheng S, Strader JH, Ma E, Xu J. Scripta Mater 2007;56:161.
[50] Lee CJ, Huang JC, Nieh TG. Appl Phys Lett 2007;91:161913.
[51] Zhang ZF, Zhang H, Shen BL, Inoue A, Eckert J. Philos Mag Lett 2006;86:643.
[52] Jia P, Guo H, Li Y, Xu J, Ma E. Scripta Mater 2006;54:2165.